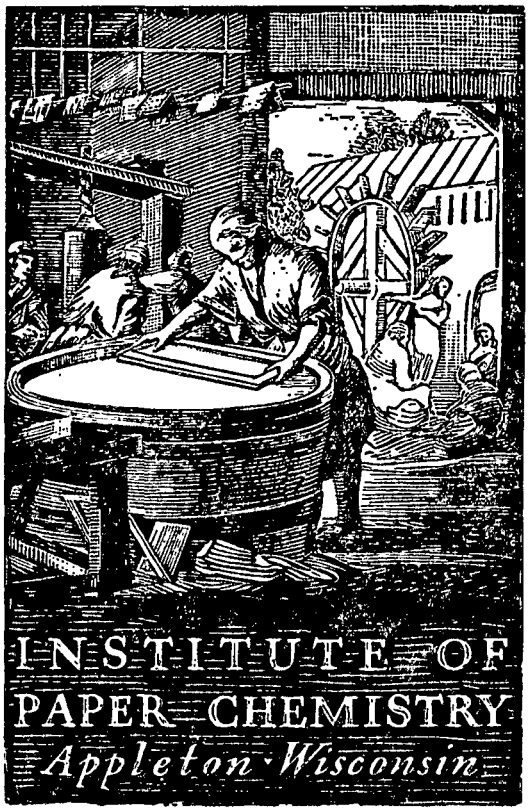

A STUDY OF THE BIAXIAL STRESS-STRAIN BEHAVIOR OF SACK PAPER

PART I. THEORETICAL CONSIDERATIONS AND DESCRIPTION OF A STATIC BIAXIAL STRESS-STRAIN TESTER

Project 2033

Progress Report Ten

to

MULTIWALL SHIPPING SACK
PAPER MANUFACTURERS

September 8, 1959

THE INSTITUTE OF PAPER CHEMISTRY

Appleton, Wisconsin

A STUDY OF THE BIAXIAL STRESS-STRAIN BEHAVIOR OF SACK PAPER

PART I. THEORETICAL CONSIDERATIONS AND DESCRIPTION OF A STATIC BIAXIAL STRESS-STRAIN TESTER

Project 2033

Progress Report Ten

to

MULTIWALL SHIPPING SACK PAPER MANUFACTURERS

September 8, 1959

TABLE OF CONTENTS

	Page
SUMMARY	1
INTRODUCTION	4
THEORETICAL CONSIDERATIONS	9
DESCRIPTION OF BIAXIAL STRESS-STRAIN TESTER	20
Apparatus Imposing Deformation on the Specimen	25
Measurement of Load	30
Measurement of Deformation	33
CALIBRATION OF BIAXIAL TESTER	34
LITERATURE CITED	43

THE INSTITUTE OF PAPER CHEMISTRY

Appleton, Wisconsin

A STUDY OF THE BIAXIAL STRESS-STRAIN BEHAVIOR OF SACK PAPER

PART I. THEORETICAL CONSIDERATIONS AND DESCRIPTION OF A STATIC BIAXIAL STRESS-STRAIN TESTER

SUMMARY

It is evident from experiment and everyday observation that filling, handling and impacting of a multiwall sack subjects the sack paper to stresses and strains in both the machine and across-machine directions of the paper simultaneously. The behavior of sack paper under the action of combined stresses, however, has not been established. Many of the conventional sack paper tests are one-directional (uniaxial) tests and, therefore, provide no direct information on the behavior of the paper when it is subjected in service to stresses in two directions (biaxial). Those several biaxial sack paper tests which are employed in the industry are not readily interpretable in terms of the fundamental stress-strain behavior of the paper.

Experience with a wide range of materials other than paper has been that biaxial tension is characterized by three effects, relative to the uniaxial tensile properties of the material: (a) increase in apparent stiffness, (b) decrease in stretch, and (c) tensile strength related to, but not necessarily equal to, the uniaxial tensile strengths. Accordingly, it is possible that conventional uniaxial strength data for sack paper may require additional interpretation to be meaningful in service applications where the sack is subjected to biaxial stresses and strains.

A review is presented in this report of several theories of strength which attempt to describe the relationship between strength under combined stresses and uniaxial strengths for various classes of materials.

A fundamental study has been undertaken to determine the behavior of sack paper under combined stresses, with particular interest centered on the ultimate strength and stretch in biaxial tension. Information of this type may be expected to lead to a more accurate description of sack serviceability and improved selection and specification of sack paper properties.

The initial phase of this study has been concerned with development of adequate test methods for measuring the biaxial tension properties of sack paper. A test instrument was designed and constructed whereby a sack paper specimen may be subjected to arbitrary tensile stresses or strains in two perpendicular directions simultaneously, with provision for continuously measuring the tensile loads and deformations in each direction.

A sack paper specimen having six-inch square dimensions (or less) is secured in four clamps along its boundaries. Each pair of opposite clamps is caused to move apart by turning a handwheel on a threaded shaft. Tension force in either direction of the specimen is measured by means of electrical resistance strain gages mounted on the clamp assembly and is recorded with a strip chart potentiometer. Two load ranges are provided--0 to 300 lb. and 0 to 150 lb. The over-all deformation in each direction is measured by means of a dial indicator, although exploratory testing has shown the feasibility of measuring the strain over a shorter gage length at the center of the specimen with an extensometer.

The load sensing system of the biaxial tester was calibrated by means of a proving ring and found to be essentially linear and reproducible to within ± 1%.

A subsequent report will present the results of preliminary biaxial tests of sack paper.

INTRODUCTION

Experiments with multiwall sacks reveal that filling, handling, and impacting subject the sack paper to stresses and strains in two directions simultaneously (1, 2). Strain measurements on impacted sacks, for example, exhibit tension strains of the same order of magnitude in both the in-machine and across-machine directions at various locations in the sack. Furthermore, a rather favorable correlation was found in the recent fabrication studies of Project 2033 between sack impact behavior and the Couch-Muldoon sack paper test. Inasmuch as the latter test imposes a biaxial ((two-directional) stress condition on the test specimen, the favorable correlation may be attributable to a biaxial stress behavior in the paper of the multiwall sack during impact.

Unfortunately, the behavior of sack paper under biaxial stresses and strains is not adequately known. Sack paper testing is frequently limited to uniaxial (one-directional) tension, such as the conventional tensile tests or the Frag impact fatigue test. The relationship between uniaxial and biaxial tensile properties has not been established for sack paper.

In those several laboratory tests where biaxial stresses are imposed on the sack paper specimen (Couch-Muldoon or burst test, for example), the degree of simulation of sack impact stresses is obscure. Furthermore, the test result is in the nature of an index (drop number and lateral pressure for the cited examples) which is not readily

interpretable in terms of the fundamental stress-strain properties of the sack paper.

Experience with a wide range of materials reveals that biaxial tension is characterized by three effects, relative to uniaxial tensile properties:

(a) An increase in apparent stiffness. The elastic stress-strain relationships for biaxial tension (3, 4), reveal that a greater force is required (relative to uniaxial tension) to obtain a given elongation in one direction, due to the contraction which occurs in the second direction. That is, the material is apparently stiffer than in uniaxial tension.

(b) A decrease in ductility (stretch) (5).

(c) The tensile strengths are related to, but not necessarily equal to, the uniaxial tensile strengths (6, 7, 8).

Items (b) and (c) are concerned with the failure characteristics of materials subjected to tension stresses simultaneously in two directions. Depending on the magnitude of the reported effects, conventional uniaxial strength data may require additional interpretation to be meaningful in service applications where a structure is required to withstand biaxial stresses and strains.

An ever-increasing interest in determining the behavior of materials under combined stresses is evident in the literature of mechanics and is probably due to two reasons. First, there is a tendency toward an increasing complexity in design of structures, purposely requiring that the material resist combinations of stresses rather than simple stresses

in order to effect savings in weight or satisfy space limitations. Secondly, many structures, such as sacks, inherently are subjected to combined stresses; attempts to improve the precision of analysis of the behavior of these structures quite naturally lead to considerations of the material characteristics under combined stress.

Numerous theories have been formulated for the relationship between the strength of a material under combined stress and its strengths under uniaxial stress. Several of these theories are reviewed in the section of this report titled Theoretical Considerations. Paralleling the theoretical development of the subject are an array of experimental methods which have been devised for subjecting test specimens to various combinations of stresses. A review of several classical methods of imposing biaxial stresses is given in Reference (9). For example, a state of biaxial tension may be obtained with an axially loaded cylinder which is also internally pressurized. This method was employed by Anderson (10) for flexible sheet material (e.g., rubberized fabric) and by Boonstra (11) for natural rubber.

Checkland, et al. (12) adapted a four-jaw lathe chuck to impose equal deformations in two directions of fabrics and films, with provision for measuring the loads in the two directions. Reichardt, et al. (13) added a pair of lateral clamps to an Instron testing machine so that deformation may be imposed on woven fabrics in two directions in one of several fixed ratios. The Instron load-weighing system provided load measurements in one direction and a light-weight extensometer was constructed to measure deformations in one direction over a short gage length at the center of the specimen.

As may be expected, the most intensive investigations of the behavior of materials under combined stresses have been undertaken for metals. The references cited above attest to increased activity with regard to fabrics and films. No published record of investigation of the behavior of paper (or paperboard) under combined stresses is known.

As a part of the special studies of Project 2033, The Institute of Paper Chemistry initiated a fundamental study of the behavior of multiwall sack paper under the action of biaxial stresses. The first phase of this study has been concerned with development of adequate experimental methods for the determination of the biaxial tension properties of sack paper. The information acquired from testing of this type, in combination with a knowledge of the stresses and strains induced in a sack under service conditions (e.g., Reference 2), may be expected to lead to a more accurate description of sack failure. In turn, a better understanding of sack failure should enable a more enlightened selection and specification of sack paper properties.

With regard to development of biaxial testing methods, the following criteria were adopted:

(a) Provision for subjecting a sack paper specimen to progressively increasing tension in each of two directions by applying arbitrary ratios of tension force or of deformation in the two directions.

(b) Provision for measuring tensile force and deformation independently in each direction and continuously during the test.

None of the previously cited biaxial test methods satisfied these criteria fully. Therefore, a biaxial stress-strain tester was

designed and constructed. A description of this tester and its calibration is presented in this report.

THEORETICAL CONSIDERATIONS

Determination of the strength of structural materials is usually restricted to tests which impose only the very simplest types of stresses on the material, such as tension or compression in one direction or shear. On the other hand, structures fabricated from these materials frequently encounter service loads or deformations which give rise to complex combinations of stresses. Thus, while the material strength may be known for relatively simple stress conditions, the analysis of the structure may entail consideration of the strength of the material under combined stress, e.g., tension in two perpendicular directions, or tension combined with shear. To meet this need, various theories of strength have been formulated for the purpose of predicting the material strength under combined stress in terms of the simple strength properties of the material. While most of these theories were originally devised to predict inception of yielding in metals, some of them have been extended semiempirically to describe rupture.

Inasmuch as most strength theories are formulated in terms of principal stresses, it may be helpful to review this concept briefly for the case of biaxially stressed bodies. At any point in a stressed material, there are two mutually perpendicular directions (termed principal directions of stress) with which are associated the following properties (14, 15):

(a) The normal stresses (tension or compression) parallel to these principal directions are respectively the maximum stress and the minimum stress, with respect to stresses in all other directions in the material. These maximum and minimum stresses are called principal stresses.

(b) The shear stresses associated with the principal directions are zero.

Thus, regardless of how complex may be the biaxial stress field existing in the material, there is always an orientation within the material for which an element is shear-free and is acted on by the most severe and also the least severe tension or compression stresses. Moreover, the state of biaxial stress is completely defined and conveniently described by the principal stresses, thereby affording further utility to the principal stress concept.

In strict analogy with principal stresses, principal directions associated with strains may be defined, leading to the concept of principal strains. For isotropic materials (i.e., identical material properties in all directions) the principal axes of stress and of strain coincide. For orthotropic materials such as paper (which possess three characteristic perpendicular directions with regard to material properties) the two types of principal axes do not coincide, in general.

Returning to consideration of strength theories, a convenient representation of the theory is accomplished by means of an interaction curve. For purposes of discussion, a hypothetical interaction curve for the biaxial strength of sack paper is shown in Fig. 1. It is assumed in this example that the uniaxial in-machine tensile strength is 30 lb./in. and the across-machine strength is 20 lb./in. Each point on the interaction curve represents failure of the sack paper under combined tensile stresses applied simultaneously in the in- and across-machine directions (these stresses are assumed to be principal stresses). The coordinates of any point P on the curve are the tensile loads in each direction which will cause rupture of the paper. For example, the illustration shows that when 10 lb./in. is applied in the across-machine

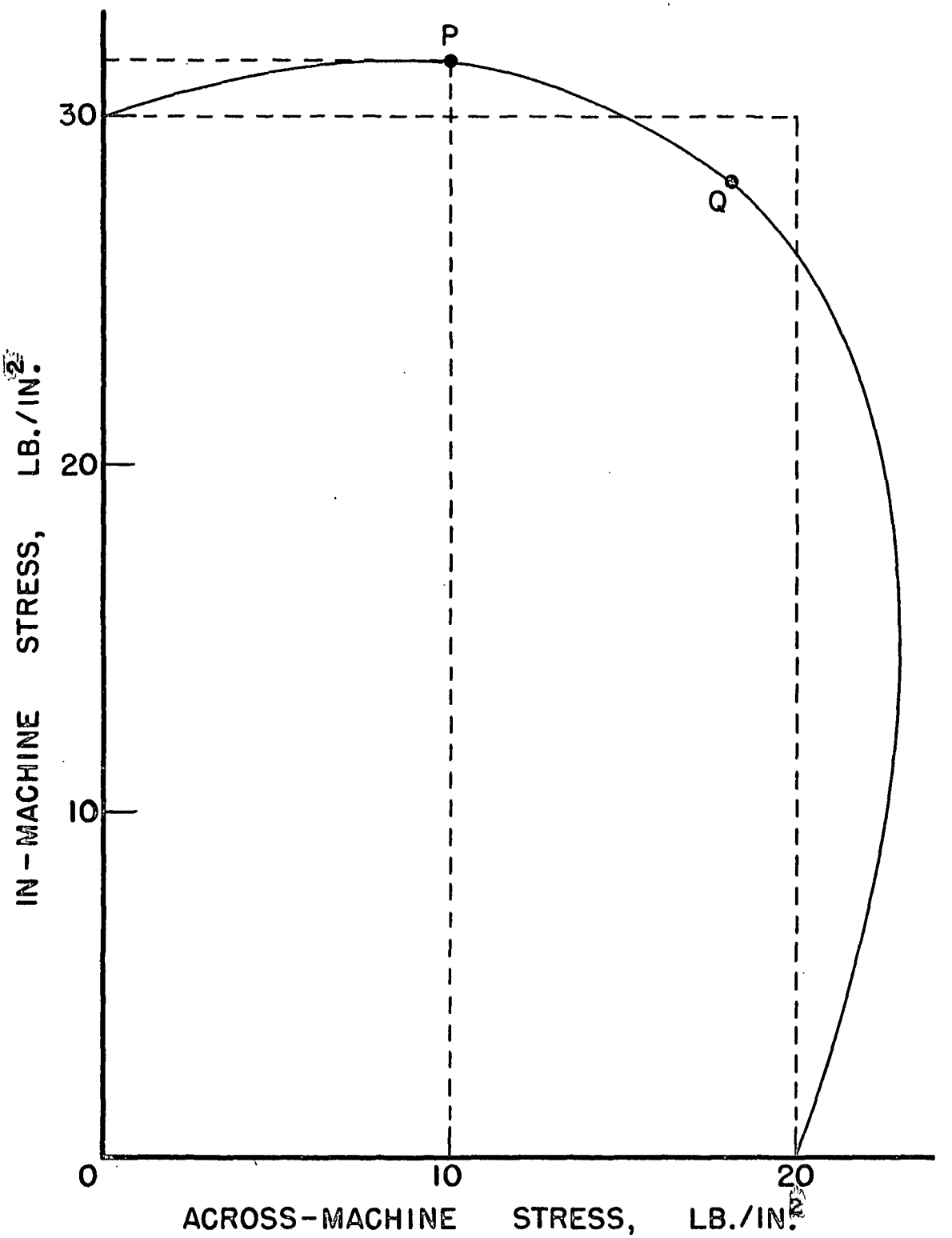

Figure 1

Hypothetical Interaction Curve for Biaxial Strength of Sack Paper

direction (one-half of the uniaxial across-machine tensile strength), the load in the machine direction (about 32 lb./in.) exceeds the in-machine uniaxial strength (30 lb./in.). In another portion of the interaction curve, such as at Q, it may be noted that the allowable stresses are respectively less than the uniaxial strengths.

The role of the strength theories is to describe analytically the failure interaction curve, such as the hypothetical curve of Fig. 1, in terms of the uniaxial strengths and with sufficient generality as to be applicable to wide classes of materials. Furthermore, the theories treat combinations of compression and tension, which amounts to describing the interaction curve in all four quadrants, rather than the single quadrant pictured in Fig. 1.

Discussions of four strength theories of both historical and practical interest is presented in References (6) and (7). These theories pertain to yielding of isotropic materials. Figure 2 presents the four interaction curves. The square (long dashed line) is the maximum stress theory, which predicts simply that the material will yield when the greatest principal stress equals the yield stress in simple uniaxial tension. This theory is sometimes employed with brittle materials such as cast iron or glass.

The rhombus (short dashed line) of Fig. 2 is the maximum strain theory, which is analogous to the maximum stress theory, but in terms of strain. This theory is not held in high repute for lack of experimental confirmation.

The irregular hexagon of Fig. 2, which coincides with the maximum stress theory in the first and third quadrant, is the maximum shear theory.

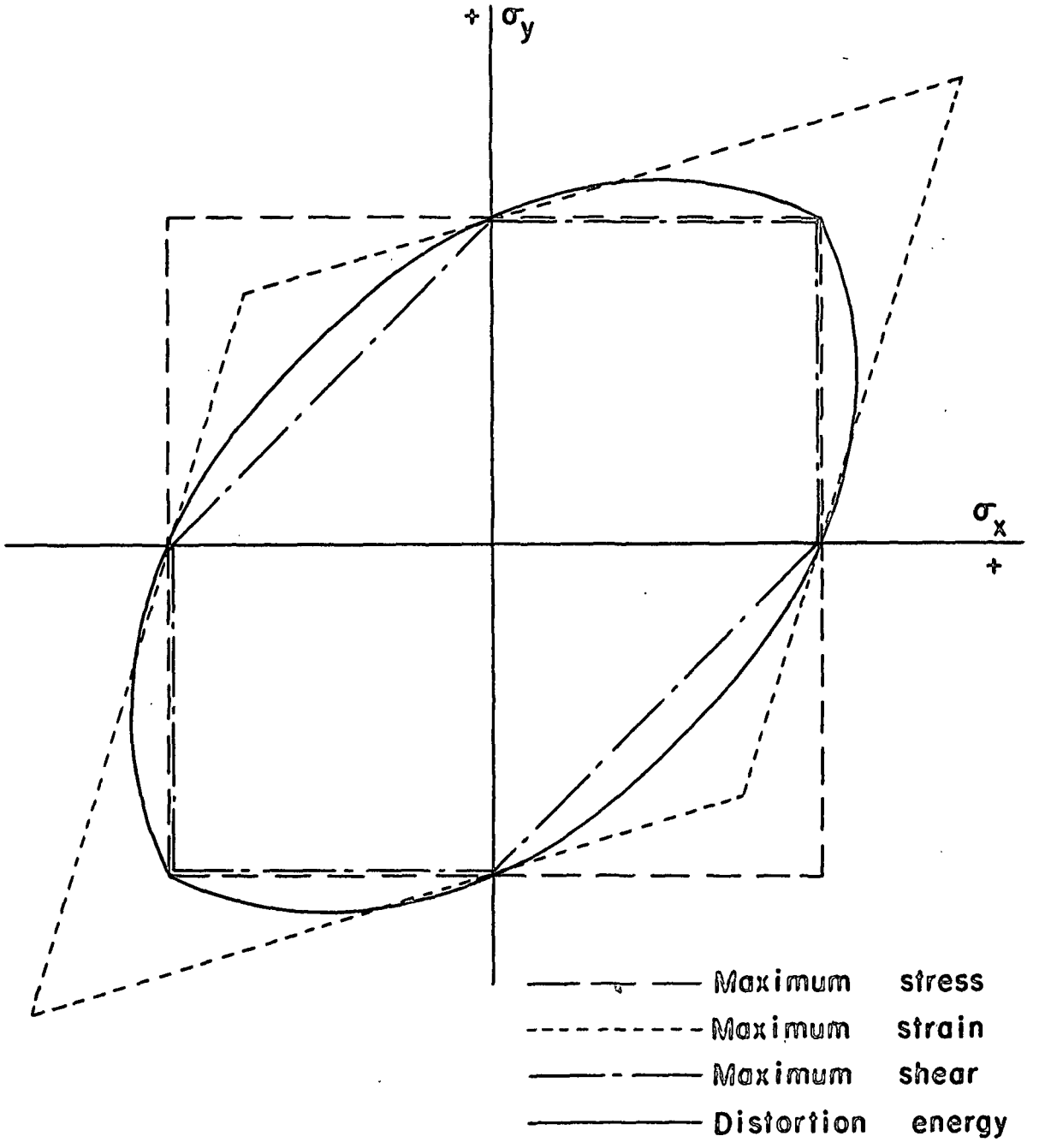

Figure 2

Interaction Curves Corresponding to Four Theories of Strength of Isotropic Materials

[From References (6) and (7)]

This theory is based on the hypothesis that the material yields when the maximum shear stress under biaxial stresses equals the maximum shear stress at yield in the simple tensile test. It may be seen that a combination of tension and compression produces marked decreases in strength relative to the uniaxial strengths of the material. This theory is widely used for ductile materials, both for its analytical simplicity and agreement with experiment.

The ellipse of Fig. 2 is the distortion energy theory (a modification of an earlier theory called the maximum strain energy theory). This theory is also widely used for ductile materials and is supported by experimental evidence.

Recently Marin (7) has proposed a generalized theory of strength which purportedly is applicable at both yield and rupture for anisotropic materials having different strengths in tension and compression. Figure 3 is a graph of Marin's theory applied to sack paper from Run A-3 of the recent fabrication study--a run widely used in the instrumentation studies of Project 2033. In the absence of compression strength data for this sample of sack paper, the tensile and compression strengths were assumed to be equal for this illustration. The Marin interaction curve is a function of three material strength properties: the tensile strengths in the machine and across-machine directions and shear strength (corresponding to shear strain in the plane of the paper). The tensile strengths for this sample of sack paper were 30.7 and 18.8 lb./in. for the in- and across-directions, respectively. Inasmuch as no shear strength data were available, four assumed values were chosen and each of the four resulting interaction

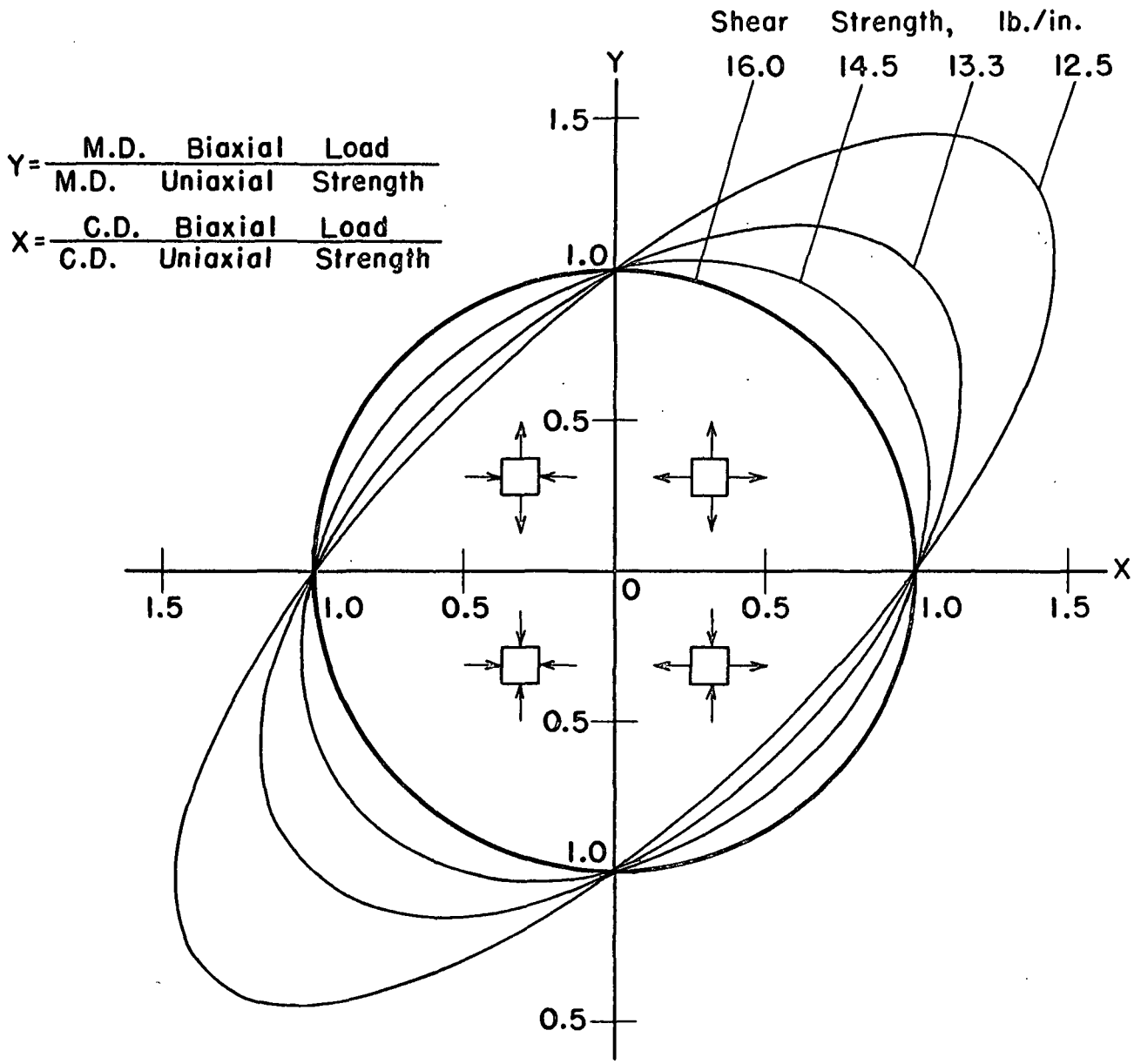

M.D. Uniaxial strength = 30.7 lb./in.
C.D. Uniaxial strength = 18.8 lb./in.

Figure 3

Generalized Theory of Strength [Reference (7)] Applied to Run A-3 Sack Paper

(for Several Assumed Values of Shear Strength)

curves is so labeled in Fig. 3. In this graph it is convenient to express the applied stress as ratios of the uniaxial strengths. Thus, all of the curves intersect the axes of the graph at 1.0.

An interesting aspect of this theory is that the biaxial strength for combined tension (or compression) decreases with increasing shear strength of the sack paper, as is evident from comparison of the four curves in the first quadrant of Fig. 3.

All of the aforementioned strength theories are formulated in terms of principal stresses. If the principal stresses arising from a given stress condition are parallel to the natural axes of an orthotropic material, the theories may be applied directly. If, however, the principal stresses are inclined to the natural axes, then it is necessary to determine the simple strengths of the material in the directions of the principal stresses. This is obviously inconvenient since the directions of principal stress may vary from one analysis to another.

Norris (8) presents a failure theory for normal stresses parallel to the natural axes of an orthotropic material, thereby requiring knowledge of the simple strengths only in the directions of the natural axes. Since the applied stresses are not principal stresses, in general, shear stresses are also present (in the general case.). Thus, this strength theory is represented graphically by an interaction surface, rather than an interaction curve, as pictured in Fig. 4 which is reproduced from Reference (8). The third axis (f_{12}/F_{12}) is the applied shear stress (expressed as a ratio of shear strength). The interaction surface is an ellipsoid, of which only two octants are shown

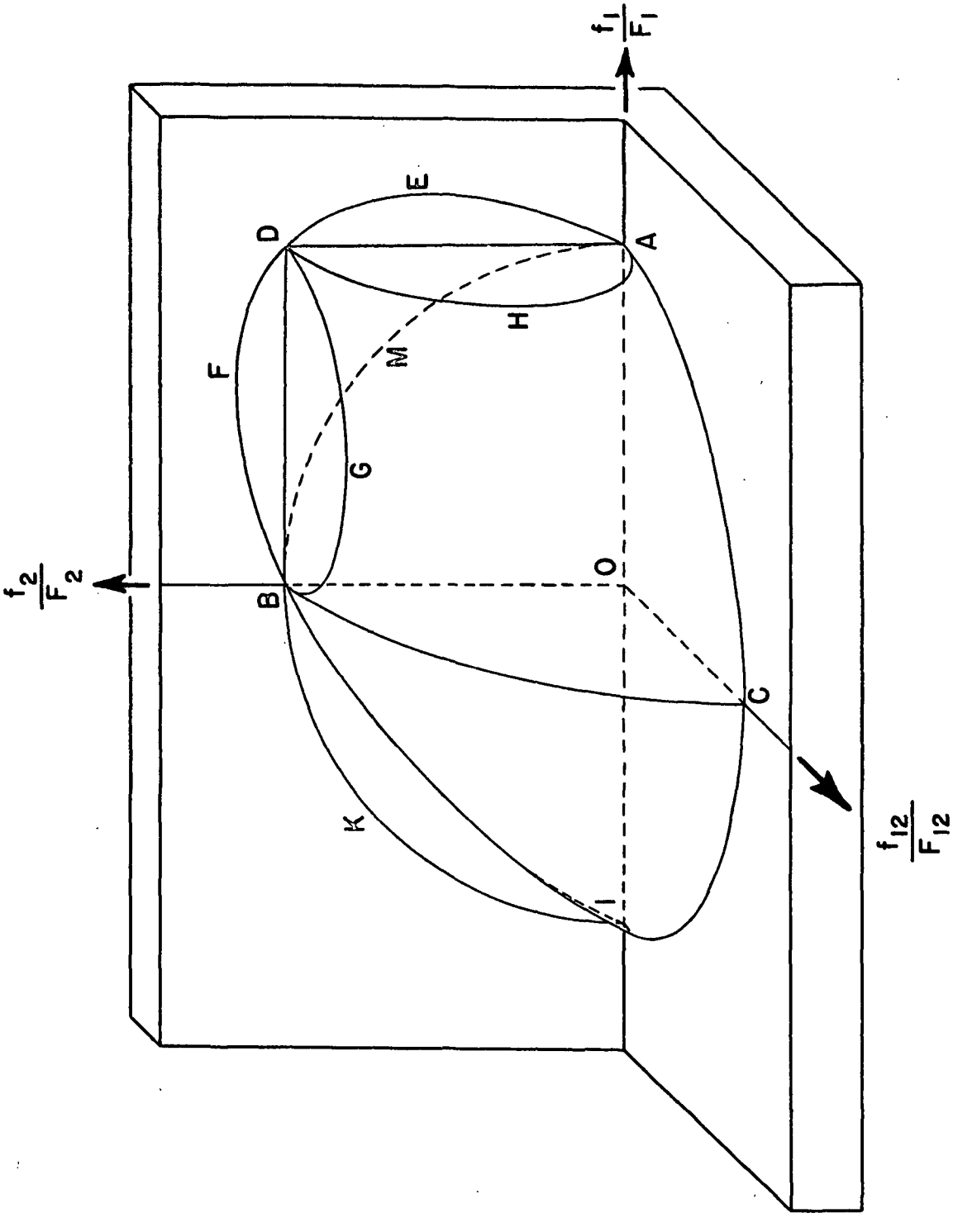

Figure 4

Theory of Strength for Orthotropic Materials [From Reference (8)]

in Fig. 4. In the first octant, however, the ellipsoid is cut off by a horizontal limiting plane through B and a vertical limiting plane through A, which points correspond to ratios of unity for the two tensile stress ratios, f_2/F_2 and f_1/F_1, respectively. This means that the biaxial tensile strength can never exceed the uniaxial tensile strengths of the material, according to this theory.

In the absence of shear stress, the interaction surface of Fig. 4 reduces to a portion of an ellipse $\overline{IB}$ in the second quadrant (as in the distortion energy theory) and to the straight lines $\overline{BD}$ and $\overline{DA}$ in the first quadrant (as in the maximum stress and maximum shear theories). The circular arc BMA in Fig. 4 is an empirical interaction curve suggested earlier by Norris.

It may be noted that for a nonzero value of applied shear stress, f_{12}, an interaction curve is obtained by passing a vertical plane perpendicular to the f_{12} axis, through the point on the axis equal to f_{12}. This plane intersects the surface in a curve which is a section of an ellipsoid in the second octant and a section of an ellipsoid and/or the limiting planes in the first octant. The biaxial tensile strength associated with this curve may be less than the uniaxial strength for sufficiently large values of applied shear stress, revealing the weakening effect which the latter has on the material strength.

Determination of an appropriate failure theory for a given material provides one ingredient for a combined stress analysis of a structure. In order to use the theory (with the exception of the maximum stress theory) one must know the ratio in which the applied stresses occur within the structure.

This ratio determines a radial line from the origin of the interaction curve. The intersection of this radial line and the interaction curve determines the magnitudes of the applied stresses which will cause failure of the material and, hence, failure of the structure.

DESCRIPTION OF BIAXIAL STRESS-STRAIN TESTER

A brief description of the salient features of construction and operation of the biaxial stress-strain tester will be followed by a more detailed discussion of the apparatus under section headings identifying the principal functional parts of the tester.

Figure 5 is a photograph of the biaxial stress-strain tester. The photograph shows four clamps (C) near the center of the tester which hold a 6 x 6-inch (7 x 7 inches over-all) sack paper tensile specimen. Each clamp is connected to a movable post (P) which is driven outward by a fine-thread screw common to a pair of opposing clamps. Turning a handwheel (H) moves a pair of opposing clamps apart from each other and thereby subjects the specimen to tensile forces in one direction. Turning both handwheels simultaneously imposes biaxial tensile stresses on the sack paper specimen.

The total force acting on the specimen in either direction of loading is measured by means of a pair of calibrated strain gages (G) mounted on a necked-down connector between a clamp and a post. The strain gage signals from the two directions of loading are switched alternately every 0.4 second to a strip chart potentiometer recorder and preserved as a nearly continuous record of tensile load.

The over-all deformation of the tensile specimen in each direction is measured by means of the dial indicators (D) mounted on the top of the clamps.

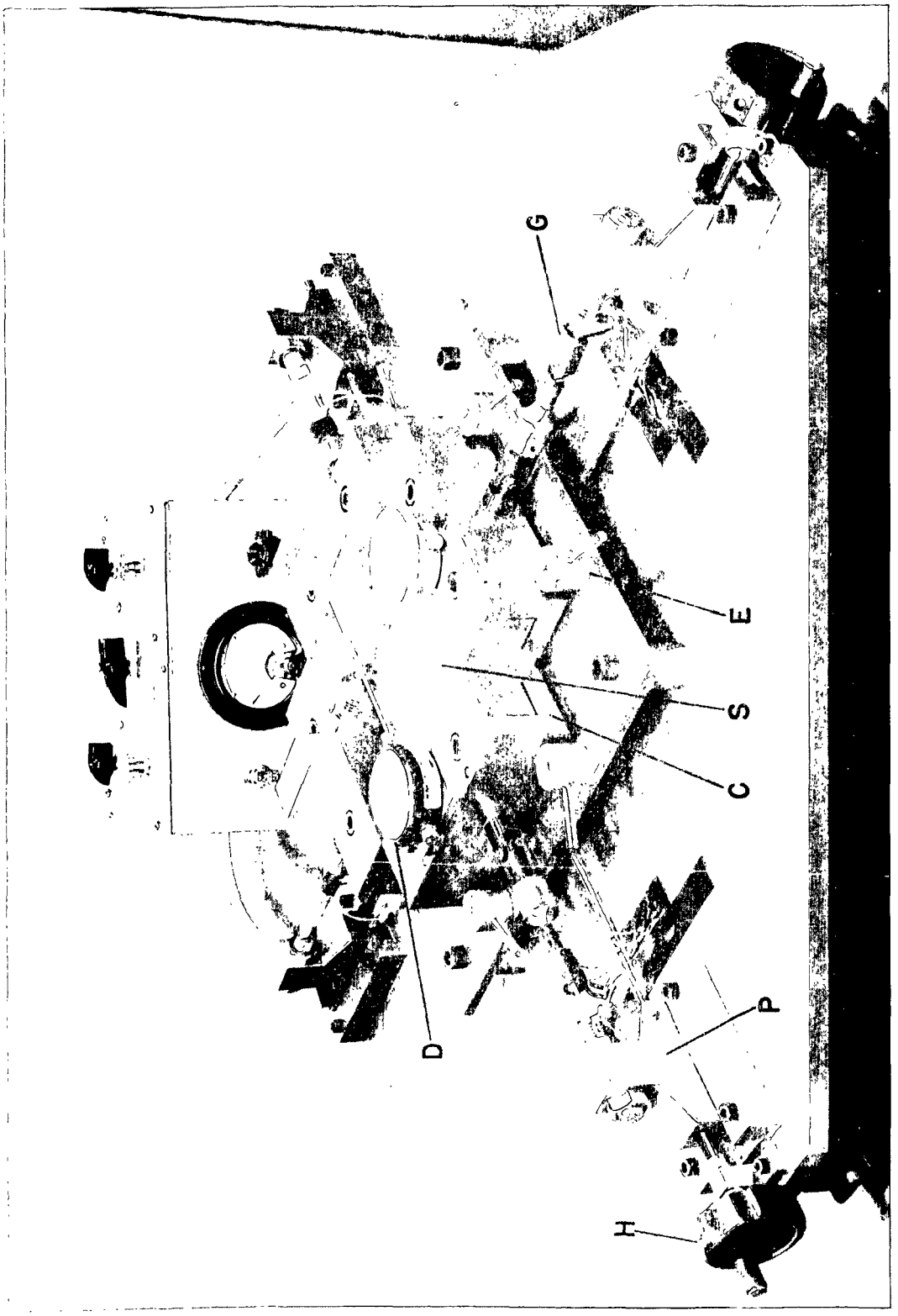

Figure 5. Biaxial Tensile Tester

A typical test procedure is as follows: The clamps are moved inward until they butt against the perimeter of a smooth 6 x 6-inch steel plate (S). They are locked rigidly against the plate by eight eccentric pegs (E). The upper half of each clamp is removed and the paper specimen is positioned on the plate with the specimen's boundaries extending into the clamping areas of the jaws which are at the same level as the top surface of the plate. The upper half of each clamp is replaced and bolted onto the lower half and the specimen is thereby clamped in place.

The eccentric pegs are thereupon removed and the loading phase of the test is begun. Both handwheels are turned simultaneously by the operator, who also inspects the dial indicators and adjusts the rate of turning so that the deformations in the two directions are in a prescribed ratio. Meanwhile, the strain gage signals (which are proportional to tensile loads) are alternately switched, by means of a motorized switch, to a recording potentiometer. At specified values of deformation, the operator actuates a foot switch which jogs a pen at the margin of the strip chart, along an axis perpendicular to the load axis. This enables the strip chart to be interpreted as a load vs. deformation curve for each direction of loading. The test is continued until the specimen has ruptured.

A variation of this test procedure permits pacing the clamp motions so that the loads in the two directions of the specimen increase according to a prescribed ratio. This is accomplished by continuously inspecting the strip chart during the test. This mode of pacing is somewhat less precise than pacing by the dial indicators and, furthermore, requires a second operator to actuate the margin pen of the recorder at given intervals of deformation.

Figure 6 is a tracing of a typical strip chart record obtained from a biaxial tension test. Load is measured along the vertical axis and time along the horizontal axis, with time increasing from right to left. The traces are purposely started at different baselines to avoid confusion between the in- and across-machine properties of the specimen. The pen trace along the upper margin of the chart is made by the aforementioned margin pen of the recorder. The distance between jogs in this instance is 0.005 inch of deformation.

The ordinates to the curves of Fig. 6 are, of course, in units of millivolts; that is, they are proportional to an electrical signal obtained from the output of the strain gages. The ordinates may be converted to pounds of force by means of the results of a calibration test, to be described later in this report.

It may be of interest to note that a recently published account of testing of rubberized fabrics (16) pictures a biaxial tester which bears a marked resemblance to the Institute tester described here. U-shaped flexural members are employed in place of the aforementioned necked-down connectors for load measurement. Details of the clamp design are not evident. The specimen is in the shape of a cross with each leg apparently six inches wide.

The remainder of this section will be devoted to a more detailed description of the biaxial stress-strain tester, in terms of its three main functional groups of components: (a) apparatus imposing deformation on the specimen, (b) measurement of load, and (c) measurement of deformation.

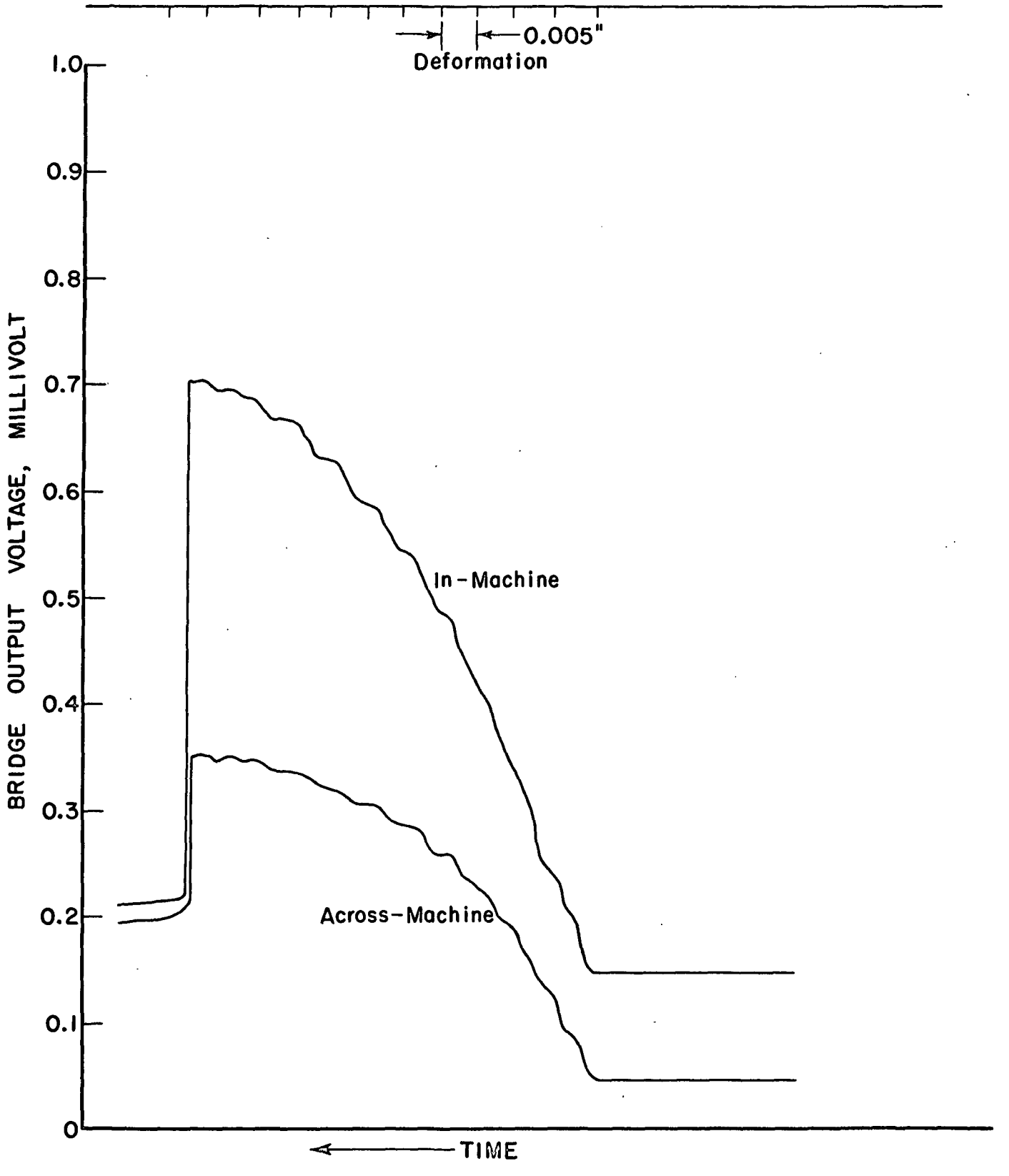

Figure 6

Typical Test Curves from Biaxial Tensile Tester

APPARATUS IMPOSING DEFORMATION ON THE SPECIMEN

Figure 7 is a plan view and sectional view of the tester, approximately to scale. The deformation-producing components are mounted on an irregular octogonal-shaped, half-inch thick steel plate, with outside dimensions of 30 x 30 inches. Mounted symmetrically at the center of the base plate is a 12-inch square, quarter-inch thick clamp table, which supports the four clamps and the 6 by 6-inch specimen table.

The specimen table was fabricated from quarter-inch thick steel plate, ground smooth on the upper surface and having tolerances of $\pm$ 0.001 inch on its side dimension and one minute of angle on the right angle between adjacent edges. The sack paper specimen rests on this smooth plate during insertion in the clamps (thereby facilitating clamping with little or no wrinkling and skewing of the specimen) and throughout the remainder of the test. It is intended that the smooth surface contacting the specimen will introduce negligible frictional forces as the specimen slides over the plate during the deformation process.

During its outward motion, each clamp rolls on three 1/4-inch steel ball bearings, retained between the 12 x 12-inch clamp table and the underside of the clamp by means of an aluminum retainer plate. The force associated with the rolling friction of the bearings and sliding of the retainer plate has been demonstrated to be negligibly small and cannot be detected by the load-measuring system.

Each steel specimen clamp is nominally 2 by 2 by 6 inches and consists of two parts. The lower element, shown in a close-up view in Fig. 8,

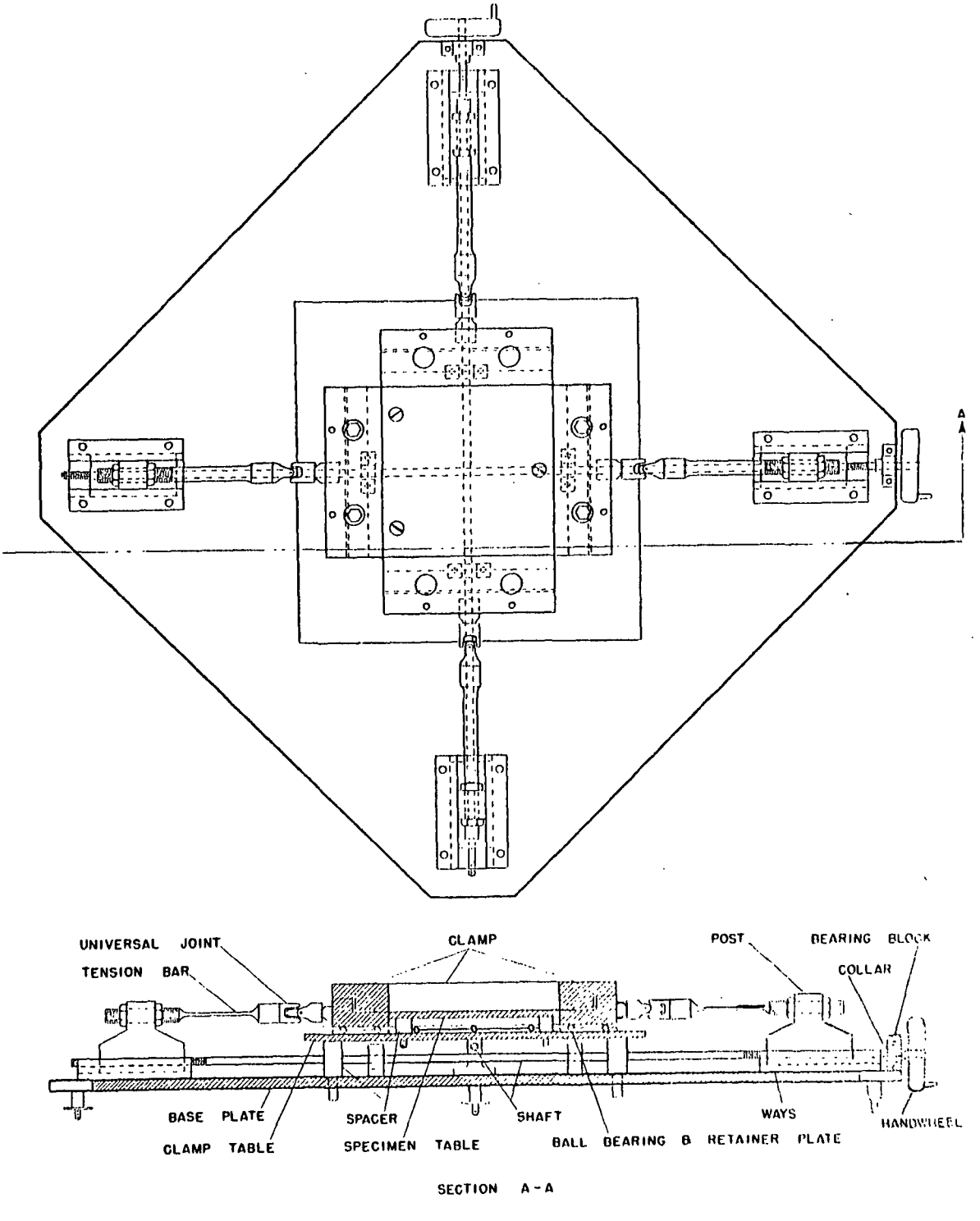

Figure 7

Plan and Sectional Views of Biaxial Tensile Tester

18

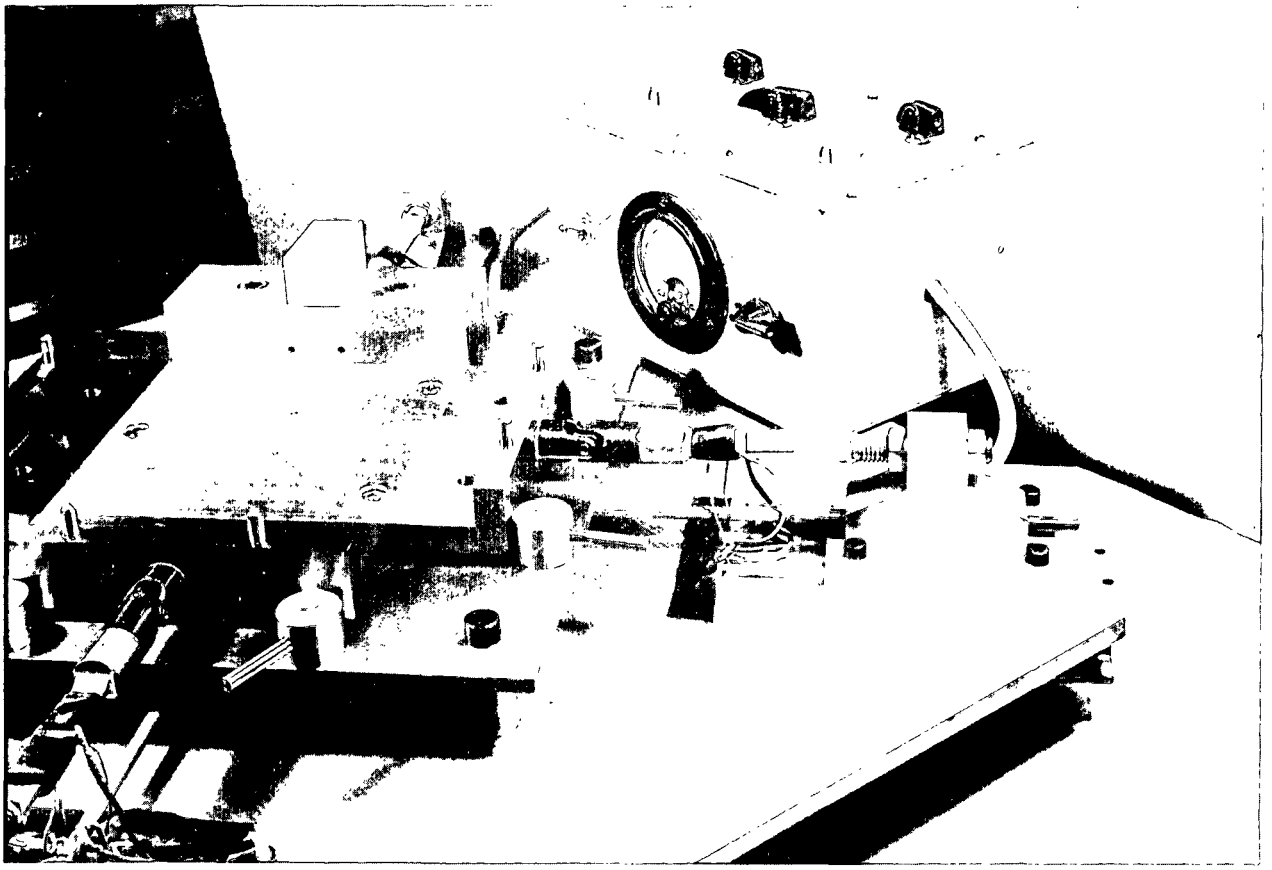

Figure 8. View of Tester with Upper Elements of Three Clamps Removed

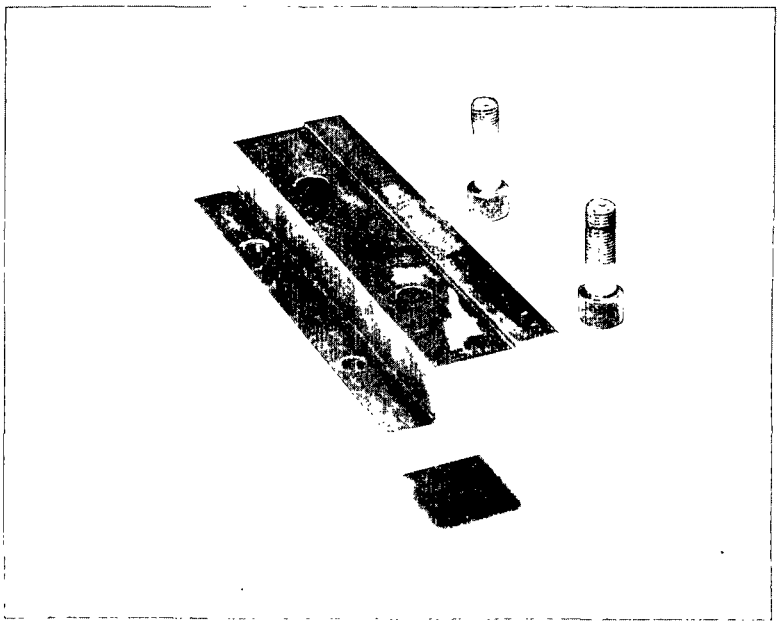

Figure 9. Upper Element of Clamp, Removed from Tester and Inverted

is permanently attached to the tester assembly. The upper element is removable for specimen insertion and is pictured in Fig. 9. Accurate mating of the two parts is accomplished by two steel pins at the rear edge of the lower clamp element. Two 1-1/8 by 3/8-inch diameter 24 NF cap screws lock the two elements together and thereby effect clamping of the specimen.

The clamping area is restricted to one-half inch of depth inward from the leading edge of the clamp and lies in the plane of the upper surface of the 6 by 6-inch specimen table. The clamping surfaces are ground. No contact between the two clamp elements exists rearward from the clamping area, except at the extreme back edge in the vicinity of the alignment pins. Here the elements again meet over a one-half inch width and along the entire rear edge. During preparation of the sack paper specimen, a strip of the paper is cut from the boundary of the specimen and placed between the clamp elements at this rear edge. This acts as a shim, having the same thickness as the specimen under test, and ensures that the clamp elements mate squarely, thereby providing a more uniform clamping of the specimen.

At the rear of the lower element the clamp is attached to pairs of connecting elements which tie the clamp to a moveable post near the extremity of the base plate. The first of these connecting units is a universal joint which permits the entire clamp to rotate about a vertical axis and a horizontal axis passing through the pins of the joint. A remark is in order on this point. Conventional tensile testers used in the paper industry usually exhibit one extreme or the other in clamp designs with regard to clamp rotation. On the one hand, an Amthor tensile tester has clamps which are constrained to move without appreciable rotation. Clamps supplied with an Instron

or a Baldwin Universal testing machine, on the other hand, have an integrally mounted universal joint which permits relatively free rotation of the clamp during the test. A merit of the rotating clamp is that it tends to remove inequalities of tensile stress which may arise at one edge of the specimen (relative to the other edge). Such inequalities may come about due to improper clamping or because of local variation in stiffness across the width of the specimen. This effect was believed to be particularly critical to the behavior of the wide specimens contemplated for the biaxial tester and accordingly the universal mounting was selected for its design.

To the rear of the universal joint is a necked-down connector (tension bar) on which are mounted two electric resistance strain gages. These are components of the load-measuring system and will be discussed in detail later in this report.

The connector is attached to a moveable post which slides in ways mounted on the base plate. The sliding surfaces of post and ways were machined to a medium fit (ASA Class 3). Frictional forces between post and ways are external to the load-detecting elements of the tester, so that friction is of consequence only in regard to ease in manual operation of the apparatus.

Two opposite posts are driven apart by means of a one-quarter inch shaft threaded with a left-hand thread at one post and a right-hand thread at the opposite post. These threads are micrometer threads--eighty threads to the inch. One revolution of the shaft, therefore, moves each clamp outward 0.0125 inch, that is, a total separation of clamps amounting to 0.025 inch. Approximately one inch of thread is engaged in each post. The shaft is supported in

3.0 1.4 turns / 1% strain · 0.0042 in/in

3

7.2

three brass-bearing blocks along its length to prevent buckling. Two collars on either side of the bearing block nearest the hand-wheel prevent longitudinal motion of the shaft.

MEASUREMENT OF LOAD

The force required to deform the specimen in either direction is transmitted from the threaded shaft to the clamps by means of the moveable posts and the connectors which link the clamps to the posts. These steel connectors are necked-down to a small cross-section (0.5 by 0.1 inch) over a portion of their length and elongate slightly under the action of these forces. Two electric resistance strain gages, mounted on the top and bottom of each connector, detect these strains in the connector and thereby serve as transducers for the measurement of tensile force in the specimen. Each pair of strain gages form opposite legs of a Wheatstone bridge. The remaining two legs of each bridge are identical strain gages and are mounted on the base plate of the testing machine to provide temperature compensation. Elongation of a connector manifests itself as an output voltage from its associated Wheatstone bridge. This output signal is recorded on a Bristol Dynamaster potentiometer recorder (0-1 mv. range) and may be interpreted as force by means of a calibration to be described subsequently.

Figure 10 is a diagram of the electrical circuits associated with measurement of tensile load. The two Wheatstone bridges at the top of the diagram are used for loads in the range of zero to 300 pounds, the high range of the load-detection system. The other two bridges detect loads in the zero to 150-pound range, the low range of the system. In either load range, one bridge

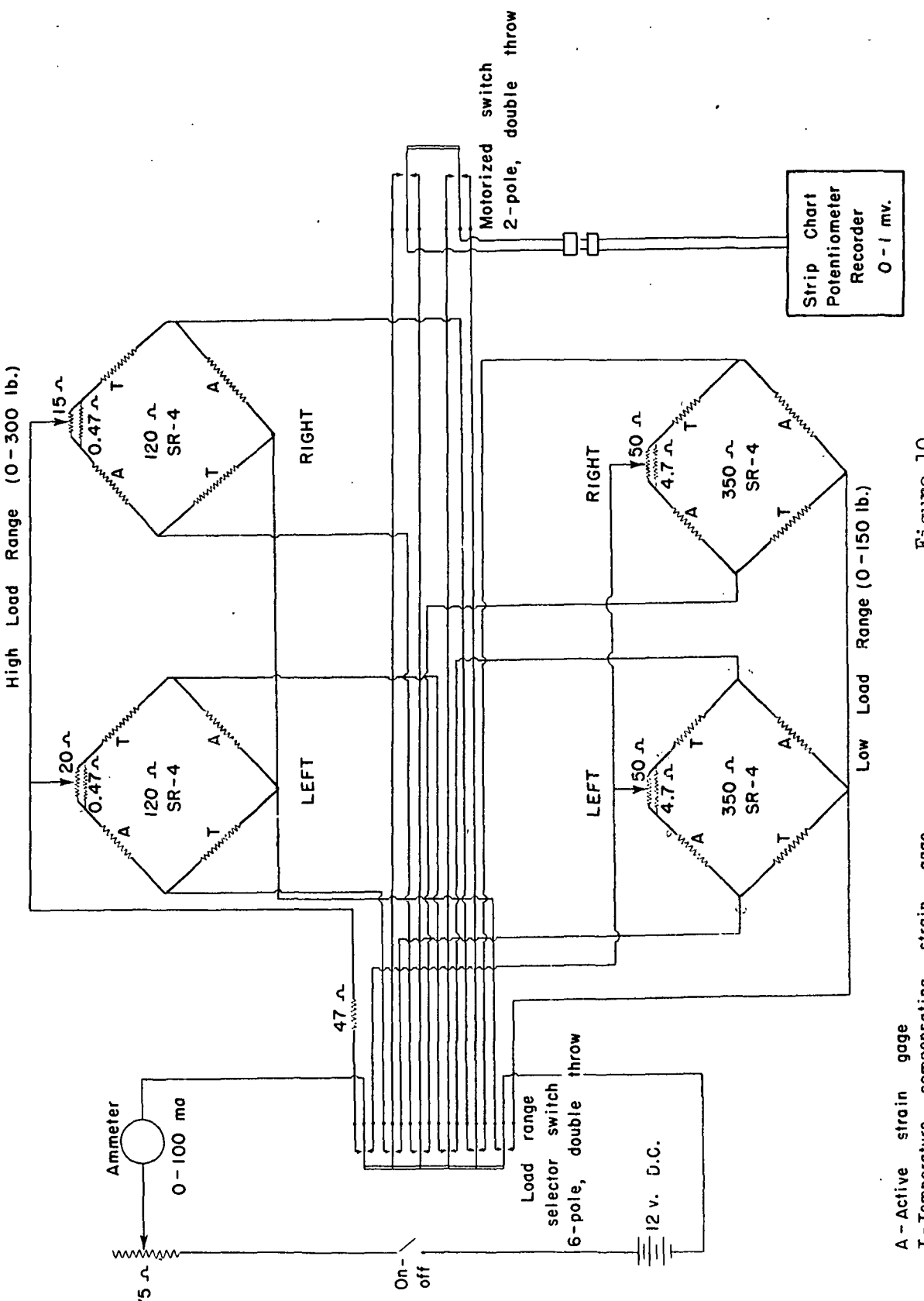

Figure 10

Electrical Circuits Associated with Measuring and Recording Tensile Test Loads of Biaxial Tester

has its active gages on a connector corresponding to the right handwheel, and the other bridge corresponds to the left handwheel. All gages of the high range are SR-4 (Baldwin-Lima-Hamilton) A-5, 120 ohms, gage factor 2.0. The low-range gages are SR-4, A-13, 350 ohms, gage factor 2.0. A variable resistor and shunt is included at one junction in each bridge to enable the bridge to be brought into initial balance.

A six-pole, double-throw, rotary switch places one or the other of the two load range circuits into the power circuit. The power circuit is comprised of (a) a 12-volt d.c. storage battery, (b) on-off switch, (c) Weston milliammeter, 0-100 ma, and (d) 0-75 ohm wire-wound, variable resistor. The variable resistor permits a degree of latitude in adjustment of the sensitivity of the bridge. The total bridge current in the high-load range may be varied from 70 to 100 milliamperes and from 50 to 66 milliamperes in the low-load range. The power circuit controls and meter, the range selector switch, and the balance controls for each of the bridges are housed in a control box mounted on the base plate of the tester, as pictured in Figs. 5 and 8.

For a given load range, the outputs from the two bridges are alternately switched to the recorder by means of a motorized, cam-operated, two-pole, double-throw switch. The switch period is approximately 0.8 second; that is, the output of a given bridge is re-admitted to the recorder every 0.8 second. The duration of signal from a given bridge is about 0.3 second. The full-scale speed of response of the potentiometer recorder is specified as 0.4 second. Since the chart distance traversed in recording consecutive bridge outputs is always less than three-quarters of full scale, the signal duration is within the speed of response of the recorder.

MEASUREMENT OF DEFORMATION

The average tensile deformation in either principal direction of the specimen is measured in terms of the displacement of the respective pairs of clamps. For this purpose, a dial indicator with spindle extension is mounted on the top surface of one clamp, with the spindle spanning the distance to the opposite clamp. The indicator parallel to the machine direction of the specimen is graduated in 0.0005 inch and has a total travel of 0.125 inch. To accommodate the higher across-machine stretch of conventional sack papers, a 1.0-inch travel dial indicator graduated in 0.001 inch is employed with the second pair of clamps.

This method of measuring specimen deformations was adopted as a temporary expedient. It is contemplated that a more refined system may be devised, such as an extensometer-type of strain transducer which will measure elongation over a limited portion of the specimen in each direction. Exploratory trials with a Baldwin strain follower, Type PS, in one direction of the specimen demonstrated the feasibility of this approach.

CALIBRATION OF BIAXIAL TESTER

Load detection in the biaxial tension tester is accomplished by means of electrical resistance strain gages mounted on linkages of the clamp drive mechanism. The forces with which the sack paper specimen resist deformation cause small elongation in the linkages, which are sensed by the strain gages and recorded on a strip chart as the voltage output of a Wheatstone bridge. The strip chart record was calibrated in terms of tensile force in the following way:

A steel proving ring was constructed, having an outside diameter of 6.15 inches, thickness of 0.1 inch, and width of one inch. A photograph of this ring is presented in Fig. 11. A dial indicator graduated in 0.0005 inch is mounted in the ring so that it measures the diametral deformation of the ring when tension forces are applied to the ring parallel to this diameter. The ring is rigidly attached to a pair of opposite clamps of the biaxial tester by means of special adapter plates which screw onto the lower elements of the clamps, after removal of the specimen table.

The proving ring itself was calibrated in a Baldwin Universal testing machine. In this test, the loads registered by the Baldwin testing machine at 0.005 inch increments of diametral deflection of the ring were noted. The load was thus progressively increased from zero to about 275 pounds, with twelve repeat trials. These repeat determinations revealed that the proving ring loads were reproducible to within $\pm$ 1% of full scale load. From these data a table of average proving ring load *vs.* dial indicator reading was constructed.

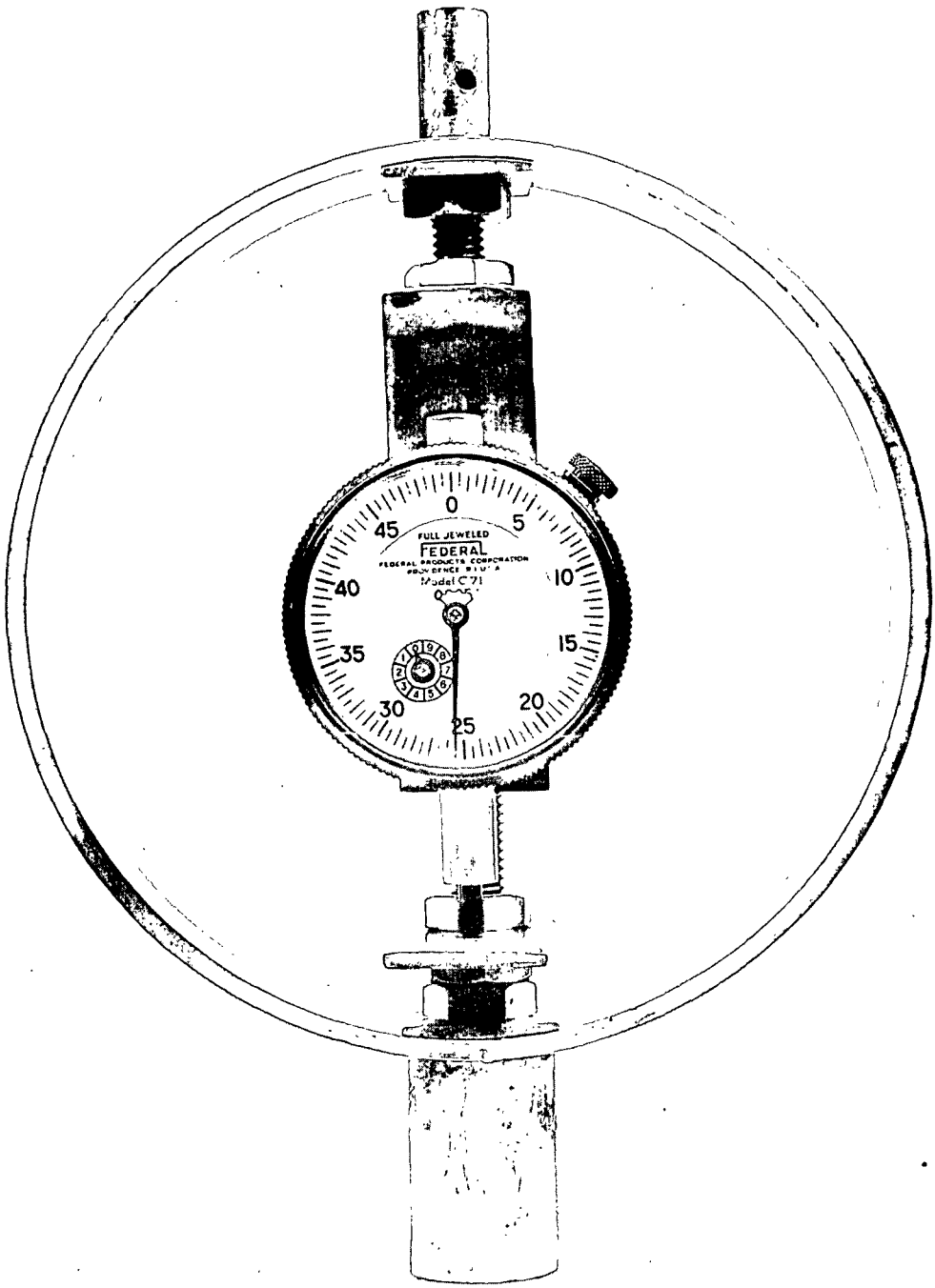

Figure 11

Proving Ring Employed in Load Calibration of Strain Gages

The proving ring subsequently was attached to a pair of opposite clamps corresponding to the right handwheel of the biaxial tester. The high-load range was selected and the bridge current set at 70 milliamperes. The clamps were moved apart so that the proving-ring dial-indicator reading changed by increments of 0.010 inch. Meanwhile, the strain gage bridge output was recorded by the potentiometer recorder. The load was incrementally increased until the safe capacity of the proving ring (about 275 pounds) was reached. This process was repeated three times. The strain gage output was found to be reproducible to within ± 1/2% of the full scale reading.

From the three replications, a table was constructed of average bridge output voltage (in millivolt) vs. proving-ring dial-indicator reading. From the data of this table and the aforementioned table, a graph was made of proving ring load vs. bridge output voltage. This constituted a calibration curve for the load-sensing strain gages in one direction of the biaxial tester, corresponding to the high-load range and 70 ma. bridge current. This curve is one of four shown in Fig. 12.

The calibration procedure was repeated for the same pair of clamps on the high-load range and with bridge currents of 80, 90 and 100 ma., yielding the remaining calibration curves of Fig. 12. It may be noted that the bridge output voltage was linear with tensile load. Accordingly, the calibration data was expressed by means of a constant calibration factor (pound/millivolt) for each of the four bridge currents. These factors are the slopes of the straight lines and are tabulated in Fig. 12. It may be seen that increasing the bridge current increased the sensitivity of the load measurement, viz. 361 lb./mv. at 70 ma. vs. 253 lb./mv. at 100 ma. This permits latitude in selecting the full-scale load on the recorder chart.

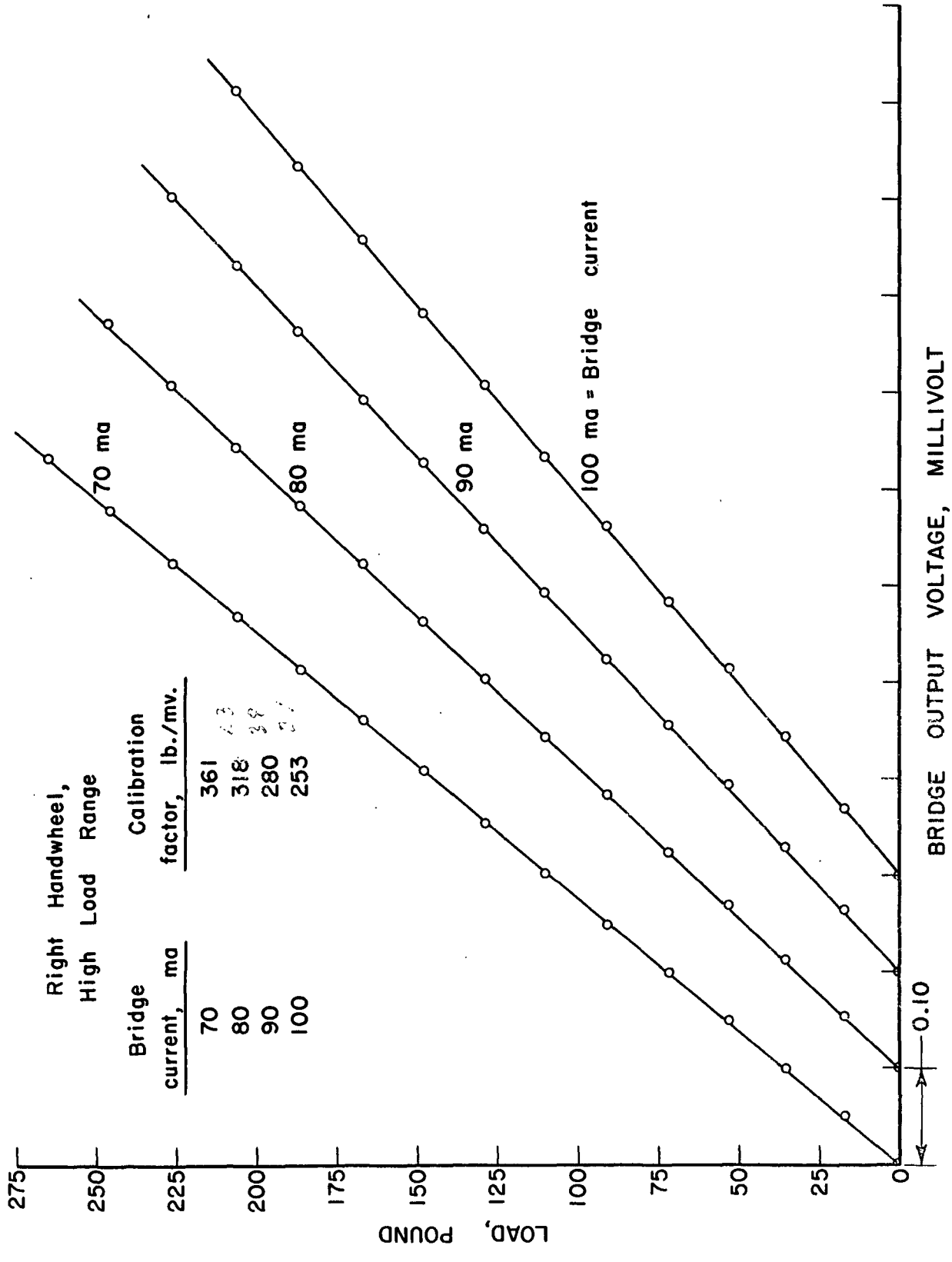

Figure 12

Load-Calibration Curves--Right Handwheel, High-Load Range

An identical calibration procedure for the second pair of clamps on the high-load range resulted in the linear calibration curves of Fig. 13.

Finally, the entire process was repeated for the low-load range at bridge currents of 50, 58, and 66 ma. These calibration data are shown in Figs. 14 and 15. Although the curves of load vs. bridge output voltage were not quite linear in this load range, the curves were approximated by straight lines and expressed in terms of the calibration factors tabulated with the curves.

As mentioned previously, the sensitivity of the load-sensing elements is continuously adjustable within either load range by changing the bridge current. To fully utilize this desirable feature, the calibration factors shown in Figs. 12 through 15 were plotted as a function of bridge current, as shown in Fig. 16. It is seen that calibration factors ranging from about 125 to 175 lb./mv. and from approximately 250 to 350 lb./mv. may be obtained by adjustment of the bridge current. For ease in the analysis of biaxial tension test data, it is possible to select a bridge current such that the calibration factor in at least one direction of the specimen is a convenient number for purposes of calculation. For example, at a bridge current of 97-1/2 ma., the calibration factors are 250 and 258 lb./mv. and at 59 ma. the factors are 140 and 150 lb./mv.

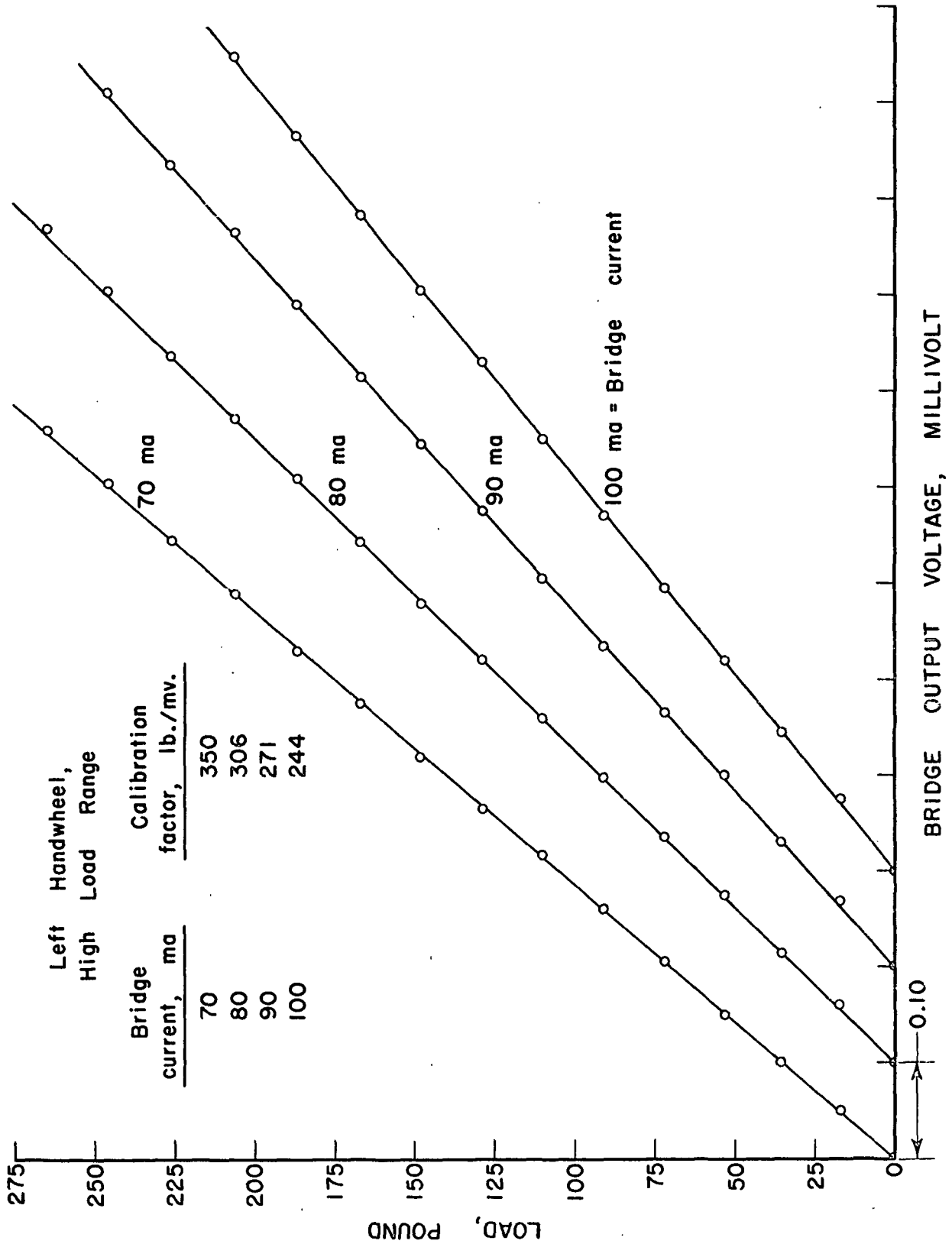

Figure 13

Load-Calibration Curves--Left Handwheel, High-Load Range

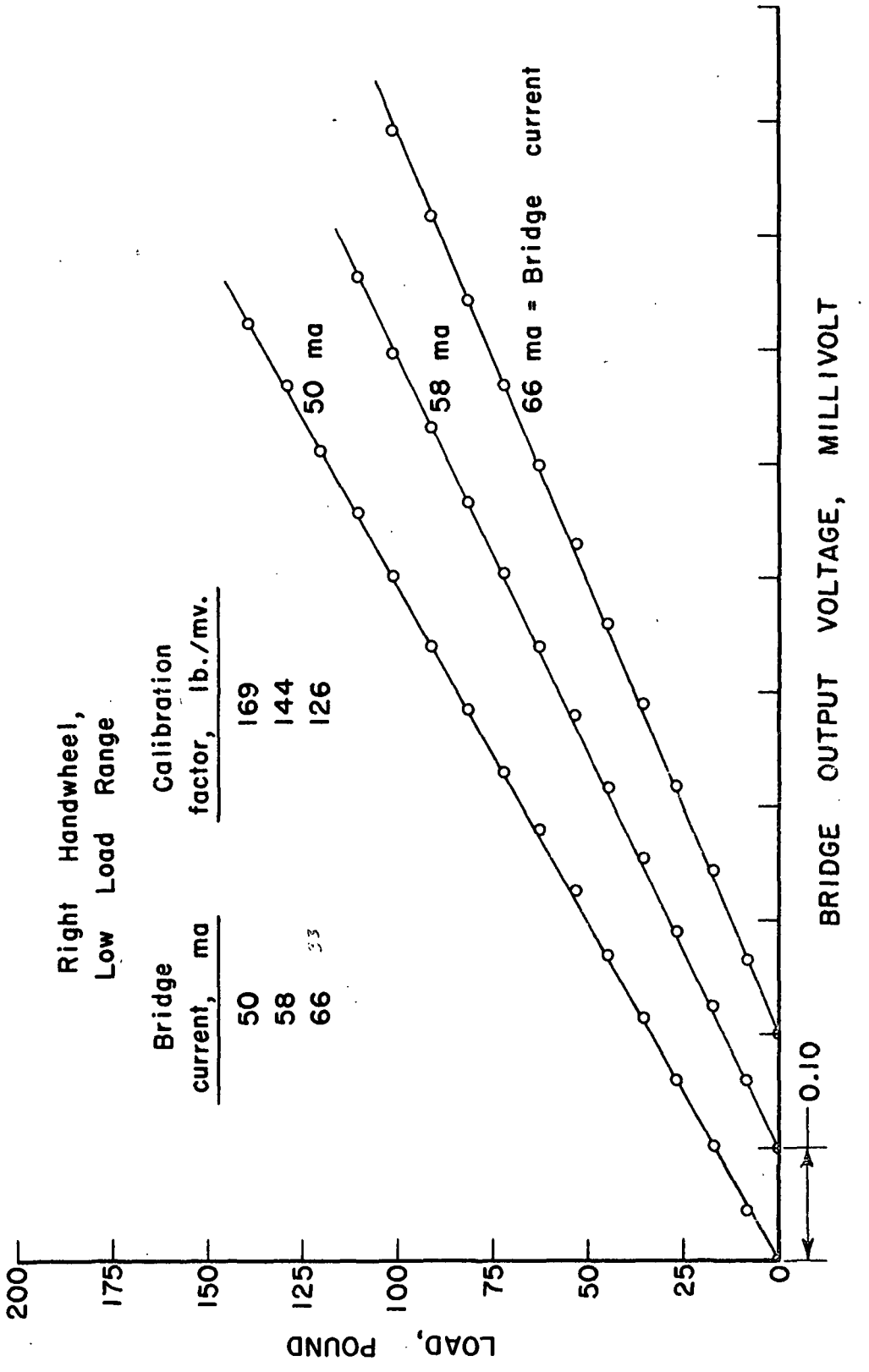

Figure 14

Load-Calibration Curves--Right Handwheel, Low-Load Range

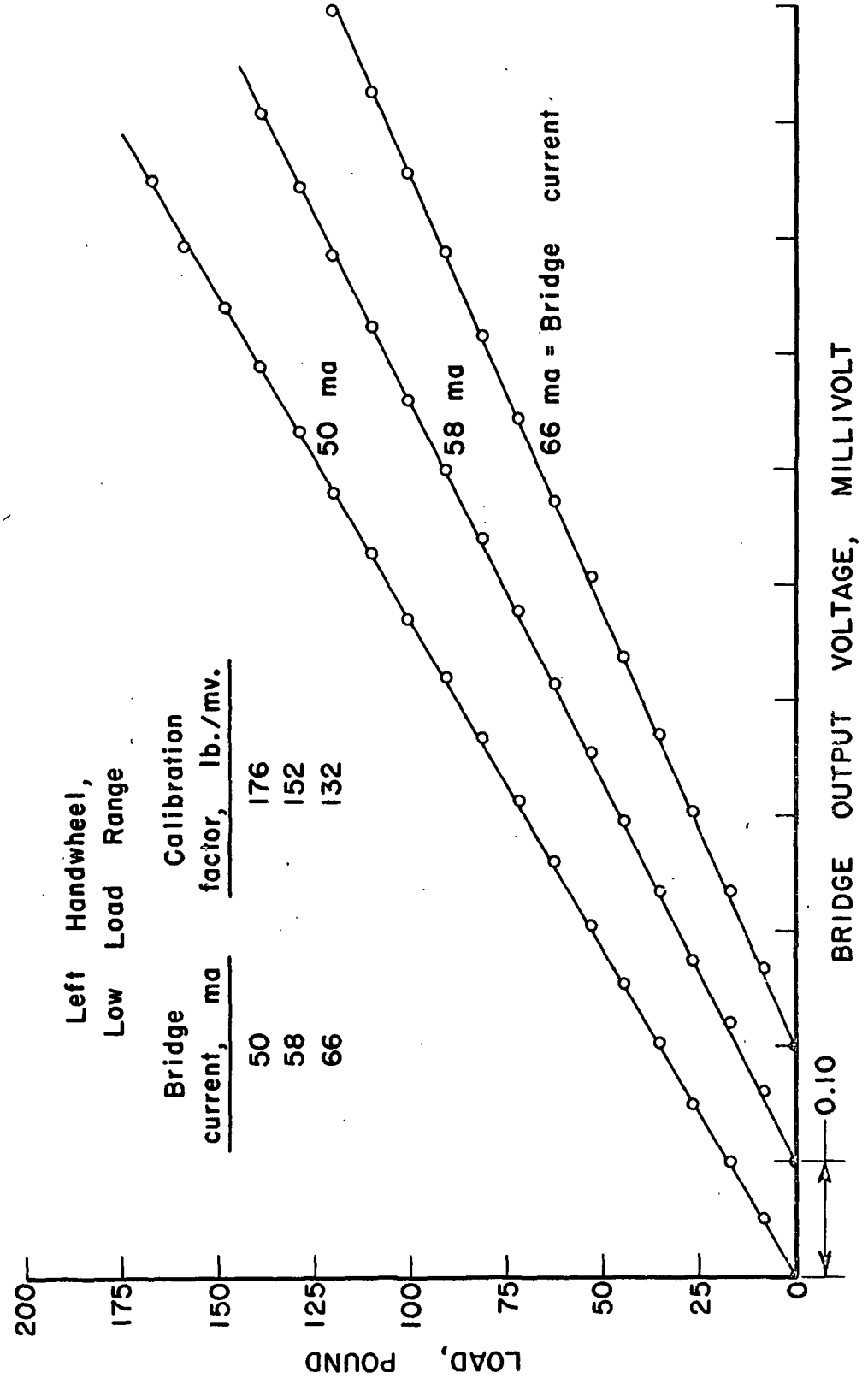

Figure 15

Load-Calibration Curves--Left Handwheel, Low-Load Range

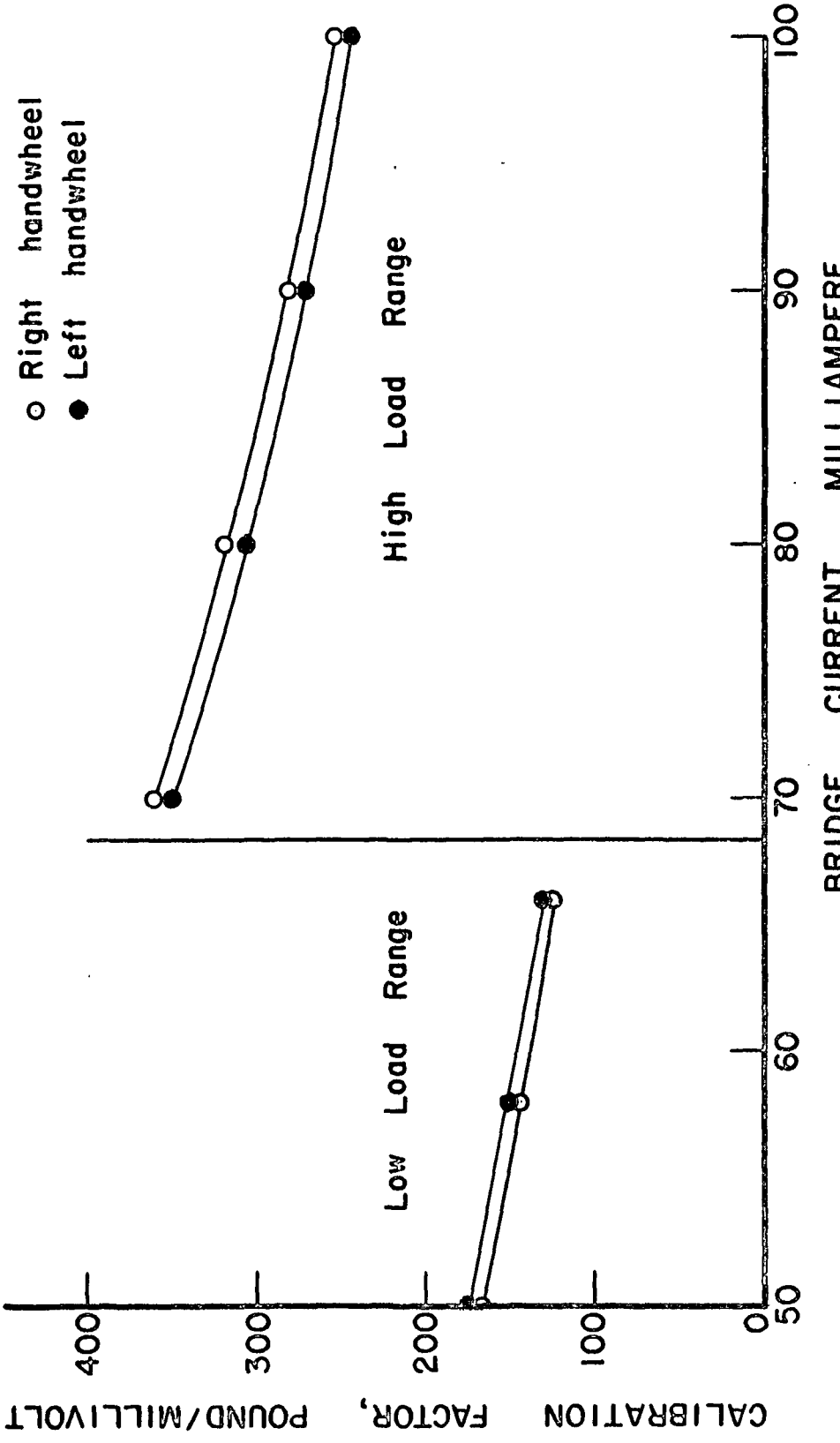

Figure 16

Graph of Load-Calibration Factor as a Function of Bridge Current

LITERATURE CITED

1. The Institute of Paper Chemistry. Effect of repeated impacts on the strength characteristics of sack paper. Project 2033, Progress Report 4, Dec. 15, 1958.

2. The Institute of Paper Chemistry. Investigation of the strains in a multiwall sack at the time of impact. Project 2033, Progress Report 8, Sept. 8, 1959.

3. Timoshenko, S. Strength of materials, Part I: Elementary theory and problems, p. 54, New York, D. van Nostrand Co., Inc. 1955.

4. March, H. W. Stress-strain relations in wood and plywood considered as orthotropic materials. Madison, Wisconsin, USDA, Forest Products Laboratory, No. R1503, Feb., 1944.

5. Marin, J. Experiments on combined stresses. Proc. Soc. for Experimental Stress Analysis 1, no. 2: 40 (1943).

6. Timoshenko, S. Strength of materials, Part II: Advanced theory and problems. p. 473. New York, D. van Nostrand Co. 1940.

7. Marin, J. Theory of strength for combined stresses and nonisotropic materials. Journal of the Aeronautical Sciences 24, no. 4:265 (1957).

8. Norris, C. B. Strength of orthotropic materials subjected to combined stresses. Madison, Wis., USDA Forest Service, Forest Products Laboratory, Report No. 1816, July, 1950.

9. See Reference 5, p. 35.

10. Anderson, S. L. Method of obtaining stress-strain relations in non-isotropic flexible sheet material under two dimensional stress. J. Sci. Instruments 24, no. 1:25-7 (Jan., 1947).

11. Boonstra, B. Stress-strain properties of natural rubber under biaxial strain. J. Appl. Phys. 21: 1028 (1950).

12. Checkland, P. B., Bull, T. H., Bakker, E. J. A two-dimensional load extension tester for fabrics and film. Textile Research J. 28, no. 5: 399-403 (May, 1958).

13. Reichardt, C. H., Woo, H. K., Montgomery, D. J. A two-dimensional load-extension tester for woven fabrics. Textile Research J. 23, no. 6: 424-8 (June, 1953).

14. See Reference 3, p. 49.

Agzi, V.D. & Isai, S.W. Anisotropic strength of composites. Experimental Mechanics 5, no. 9: 283-88, Sept. 1965 (Excellent article)

LITERATURE CITED--CONTINUED

15. Handbook of experimental stress analysis. p. 397. New York, John Wiley and Sons, 1950.

16. Baker, A., and Mikolajewski, E. Biaxial stretching of rubberized fabrics: experiments with an elliptical bursting test. J. Textile Inst. Trans. 50, no. 3: T249-T261 (March, 1959).

THE INSTITUTE OF PAPER CHEMISTRY

J. W. Gander

J. W. Gander, Research Aide
Container Section

R C McKee

R. C. McKee, Chief, Container Section